

# Theoretical Studies on How to Tune the $\pi$ -hole Pnicogen Bonds by Substitution and Cooperative Effects

Lijuan Zhang<sup>1</sup> and Dazhi Li<sup>1</sup>

<sup>1</sup>Binzhou University

July 31, 2020

## Abstract

A systemic investigation of the substitution and cooperative effects on the P...N  $\pi$ -hole pnicogen bond were performed via theoretical calculations. The structural and energetic properties of the binary complexes between a series of substituted benzonitrile and PO<sub>2</sub>F have been examined to study the substitution effect. The stability of the binary complexes increases in the order of CN

## Key Words:

Substitution effect; Cooperativity; Pnicogen bond; Triel bond;  $\pi$ -hole

## 1 Introduction

Studies of the noncovalent interactions play a vital role in fundamental research and numerous fields, such as supermolecular chemistry, crystal engineering, material science, and biochemistry<sup>[1-4]</sup>. It is generally accepted that hydrogen bond is one of the most extensively studied intermolecular interactions due to its widespread existence in various physical and chemical processes. With the development of the experimental and theoretical approaches, the role of other Lewis acid-Lewis base interactions has been discovered and investigated<sup>[5]</sup>. Amongst them, pnicogen bonds (ZBs), has been recognized as a new and important type of intermolecular interaction, where atoms from group V of the periodic table (N, P, As, Sb) act as Lewis acid centers<sup>[6]</sup>. It has been demonstrated that the pnicogen bonds can be more attractive than even several strong hydrogen bonds, which can determine the structures of the large complexes or aggregates. Owing to their diverse and potential uses in various areas, such as organocatalysis<sup>[7]</sup> and crystal materials<sup>[8]</sup>, the pnicogen bonds have recently received more and more attention in the literature concerned with its fundamentals and its applications<sup>[9-16]</sup>.

According to the  $\sigma$ -hole concept proposed by Politzer *et al.*<sup>[17]</sup>, the electrostatic component of pnicogen bonds has been explained by the regions of the positive electrostatic potential (positive  $\sigma$ -hole) interacting attractively with the negative sites on the Lewis bases. Besides, there also exist the pnicogen bond labeled as  $\pi$ -hole bonding interaction in which the region of depletion of the electron density perpendicular to portions of a molecular framework plays the role of the Lewis acid center<sup>[18]</sup>. Such pnicogen bonded complexes of PO<sub>2</sub>X (X = F, Cl) with nitrogen bases have been extensively studied by Alkorta and coworkers<sup>[19]</sup>, including the structures, binding energies and electronic properties, and it is revealed that complexation of PO<sub>2</sub>X with the strongest bases leads to P...N bonds with a significant degree of covalency. To evaluate the preference for the establishment of  $\sigma$ -hole versus  $\pi$ -hole interactions, a series of complexes involving 3rd-and 4th-row

atoms of Groups IV–VI have been studied by Frontera *et al.* [20, 21]. For the complexes between  $O_2YBr$  ( $Y=N, P, As$ ) and  $NH_3, H_2O,$  and  $HF$  acting as Lewis bases, it is revealed that the complexes in which the lone pair of the Lewis base interacts with the  $\pi$ -hole are more favorable than those with  $\sigma$ -hole [20]. For the  $\pi$ -hole bonding complex between  $IF$  and  $ZO_2F$  ( $Z=P, As$ ), it is found that the largest binding energies were obtained when the fluorine atom acts as the electron donor [21].

Although several systems with pnictogen bonding interaction have been investigated extensively, some problems are still worth studying. One of the important aspects is tuning the interaction strength of the pnictogen bond for future modelling of novel materials. One way called “covalent way” is by changing different substituents on the Lewis acid or the Lewis base [22]. In several chemical cases, the electron-donor may be bonded to different sorts of carbon chains. The effect of the length and type of the chain on the electron-accepting P atom’s ability engaging in a  $P\dots N$  bond have been investigated by Scheiner and coworkers [23]. It is found that the incorporation of  $C=C$  double bond in the chain tends to strengthen the  $P\dots N$  pnictogen bond in the  $RH_2P\dots NH_3$  complexes, and the addition of several conjugated double bonds such as aromatic phenyl ring has only a marginal further change. However, the substitution effects considered were mainly bonded to the electron-accepting P-atom. This lead to the natural question as to how might addition of various groups to the electron donor tune the pnictogen bond.

Another way to modulate the strength of the pnictogen bond is by introducing another intermolecular interaction, and the interplay between the two interactions can be referred to as “cooperative effect” [24, 25]. Understanding the relationships of these noncovalent interactions coexisting in the complexes is significant for the design of novel materials or supramolecular systems. The interplay between the pnictogen bond and regium bond in the ternary complexes  $HN_3\dots FH_2X\dots MCN$  ( $X=P, As; M=Cu, Ag, Au$ ) has been studied by Li *et al.* [26], and it is found that the pnictogen bond is strengthened through the cooperative effect with the regium bond. According to the research by Bene and coworkers [27], the presence of the  $P\dots Y$  halogen bond makes  $PH_3$  a better electron-pair acceptor in the  $XY\dots PH_3\dots N$ -base ternary complexes, which is caused by the synergistic effect between the pnictogen-bond and the halogen bond. A detailed computational analysis of the interplay between the  $\sigma$ -hole pnictogen-bonding and the aerogen-bonding interaction has been reported by Esrafilii *et al.* [15], in which favorable cooperativity is observed in  $Y\dots PH_2CN\dots ZO_3$  ( $Y = NH_3, N_2$  and  $Z=Ar, Kr, Xe$ ) complexes. Very recent calculations have noted that negative cooperative effect exists in the pnictogen bonded trimers formed by  $ZF_3$  ( $Z=P, As, Sb, Bi$ ) and a number of nucleophiles [28]. However, to our knowledge, little focus has been given to how might the  $\pi$ -hole pnictogen bond be effected by the other intermolecular interaction through cooperative effect. Herein, we focus on two typical intermolecular interactions,  $\sigma$ -hole halogen [29] and  $\pi$ -hole triel bonding interactions [30], wherein the group VII and III atoms act as the Lewis acid center.

According to the previous molecular electrostatic potential analysis,  $PO_2F$  is a good candidate to act as the electrophile in forming  $\pi$ -hole pnictogen interactions. To study the bridging role of  $\pi$ -electrons of aromatic molecule in tuning the pnictogen bonds, we chose substituted benzonitrile ( $R-Ph-CN$ ) as the Lewis bases. To study the effect of another interaction (halogen/triel bond) on the pnictogen bond,  $CN-Ph-CN$  and  $Br-Ph-CN$  are chosen as the center molecule in complexes  $X\dots CN-Ph-CN\dots PO_2F$  and  $Y\dots Br-Ph-CN\dots PO_2F$  for  $X=F_2, Cl_2, Br_2, FCl, FBr, BrCl, FCN, ClCN, BrCN, BH_3, BF_3,$  and  $Y=NH_3, NH_2CH_3, NHCH_2, HCN$ . In the present paper, the binary complexes  $R-Ph-CN\dots PO_2F$  ( $X=H, F, Cl, Br, CH_3, NH_2, CN$ ), and a series of ternary complexes with pnictogen bond and halogen/triel bond are studied to deepen the understanding of the substitution effect and cooperative effect on the pnictogen bonding interaction. The quantum theory of atoms in molecules (QAIM), the molecular electrostatic potential (ESP), and natural bond orbitals (NBO) approaches were employed to investigate the structural and bonding properties, as well as the evolution of the pnictogen bonding interaction formed between the above complexes.

## 2 Computational Details

All theoretical calculations were performed *via* the Gaussian 16 suite of programs<sup>[31]</sup>. The dispersion-corrected density functional theory (DFT-D3) methods were used to study the systems we chose. The structures of all the monomers and the complexes included in this study were fully optimized at the B3LYP-D3/6-311+G(d,p) level of theory. The vibrational frequencies of the optimized structures were carried out at the same level and used to obtain the zero-point vibrational energy (ZPE). All stationary points were characterized as a local energy minimum on their potential energy surfaces by verifying that all the corresponding frequencies were real. The interaction and the binding energy were obtained using the double-hybrid functional method B2PLYP-D3 with jun-cc-pVTZ as the basis set. Both B3LYP-D3 and B2PLYP-D3 methods used in present study are all DFT methods including a version of Grimme’s D3 dispersion model (DFT-D3)with BJ-damping<sup>[32, 33]</sup>. Due to the inclusion of both long and medium-range dispersion effects, these DFT methods have been widely used and show generally satisfactory performance in the calculations of non-covalent interactions in similar systems<sup>[34-36]</sup>. Jun-cc-pVTZ is a modified version of aug-cc-pVTZ by removing its *f*-type diffusion basis function. This modification significantly facilitates the convergence of the geometry optimization process while the loss of accuracy is trivial<sup>[37]</sup>.

The interaction energy, denoted by  $\Delta E_{\text{int}}$ , is defined as the difference between the complex and the sum of energies of monomer whose geometries come from the optimized structure of the complex. As for the binding energy, denoted by  $\Delta E_{\text{bin}}$ , the energy of the monomer used as the reference point is derived from the energetic minima of the isolated monomers. The deformation energy, denoted by  $E_{\text{def}}$ , is calculated as the difference between  $\Delta E_{\text{bin}}$  and  $\Delta E_{\text{int}}$  of the complexes, which is the energy difference between the monomers in their equilibrium geometries and at their relaxed geometries in the complexes, and its value is positive since the complexation results in changes of the structure of monomers<sup>[38, 39]</sup>. The basis-set superposition error (BSSE) was obtained using the counterpoise correction method proposed by Boys and Bernardi<sup>[40]</sup> to correct both  $\Delta E_{\text{int}}$  and  $\Delta E_{\text{bin}}$ . The total interaction energy in the ternary system, denoted by  $\Delta E_{\text{(ABC)}}$  or  $\Delta E_{\text{total}}$ , is calculated as the difference between the energy of ternary complex and the energy sum of the monomers which is frozen in the geometry of the ternary complexes. The cooperative effects can be explained by the many-body interaction analysis<sup>[41, 42]</sup>. The two-body terms, denoted by  $\Delta E_{\text{(AB)}}$ ,  $\Delta E_{\text{(BC)}}$ , and  $\Delta E_{\text{(A-C)}_{\text{far}}}$ , are defined as the difference between the energy of each binary system and the energy sum of the monomers, which come from the geometry of ternary complexes. The interplay between the two interactions in the ternary can be estimated with the cooperative energy, denoted by  $E_{\text{coop}}$ , which are obtained by the following formulas:  $E_{\text{coop}} = \Delta E_{\text{(ABC)}} - \Delta E_{\text{(AB)}} - \Delta E_{\text{(BC)}} - \Delta E_{\text{(A-C)}_{\text{far}}}$ . This methodology has been widely used to study how the different interactions affect each other in the complexes<sup>[43, 44]</sup>.

Molecular electrostatic potentials (MEPs) maps of the isolated monomer were calculated with the Wave Function Analysis-Surface Analysis Suite (WFA-SAS) program<sup>[45]</sup> at the B3LYP-D3/6-311+G(d,p) level on the 0.001 a.u. contour of electronic density to locate the position and the value of the minima and maxima. To unveil the nature of the intermolecular interactions, the atoms-in-molecules (AIM) topological analysis were carried out with the use of the Multiwfn package<sup>[46]</sup> based on the wavefunctions generated at the B3LYP-D3/6-311+G(d,p) level. The following characteristics of bond critical points (BCPs) corresponding to the intermolecular interaction were analyzed including the electron density ( $\rho_{\text{BCP}}$ ), the Laplacian of the electron density ( $[\nabla^2]_{\text{BCP}}$ ), and the electronic energy density ( $H_{\text{BCP}}$ ), which is decomposed into electronic kinetic energy density ( $G_{\text{BCP}}$ ) and the electronic potential energy density ( $V_{\text{BCP}}$ ). The Visual Molecular Dynamics (VMD) program<sup>[47]</sup> was applied to visualize the weak interaction. The natural bond orbital (NBO) analysis was performed *via* the NBO 3.1 program<sup>[48]</sup> implemented in Gaussian 16 to estimate the orbital-orbital interactions as well as charge transfer (CT).

## 3 Results and Discussion

### 3.1 Substitution Effect on the pnicoen bond

#### 3.1.1 MEPs analysis

To better understood the structure of the complexes, the MEP analysis was performed for the selected molecules. The MEP maps of  $\text{PO}_2\text{F}$  and Ph-CN are illustrated in Figure 1, in which the most positive regions are designated by a red color. Due to the similar profile as Ph-CN, the MEP maps of a series of substituted benzonitrile R-Ph-CN (R=F, Cl, Br,  $\text{CH}_3$ ,  $\text{NH}_2$ , CN) we studied are all given in Figure S1 of Supporting Information. The values of the most positive and negative electrostatic potential ( $V_{\text{max}}$  and  $V_{\text{min}}$ ) in the isolated monomers are listed in Table 1. It is observed that there is a  $\pi$ -hole (red region) on the outermost portion of the P surface, which are perpendicular to the molecular framework. The  $\pi$ -hole value ( $V_{\text{max}}$ ) is 61.59 kcal/mol for the P atom in  $\text{PO}_2\text{F}$  monomer, and this enables  $\text{PO}_2\text{F}$  to form a  $\pi$ -hole pnicoen bond as a strong Lewis acid with R-Ph-CN compounds. As for the isolated R-Ph-CN molecules, the electron-donating group shifts the electron density towards the CN side, and this results in the potential associated with the N atom becomes more negative. The absolute value of  $V_{\text{min}}$  on the N atom increases with respect to substituent R in the order of  $\text{CN} < \text{Br} < \text{Cl} < \text{F} < \text{H} < \text{CH}_3 < \text{NH}_2$ . Here, the power of electron-withdrawn of the halogen substituents is a little different from the previous report for small molecules<sup>[49]</sup>.

$\text{PO}_2\text{F}$	Ph-CN	Br-Ph-CN	CN-Ph-CN
$\text{Cl}_2$	ClBr	ClCN	$\text{BH}_3$
$\text{BF}_3$	$\text{NH}_3$	HCN	

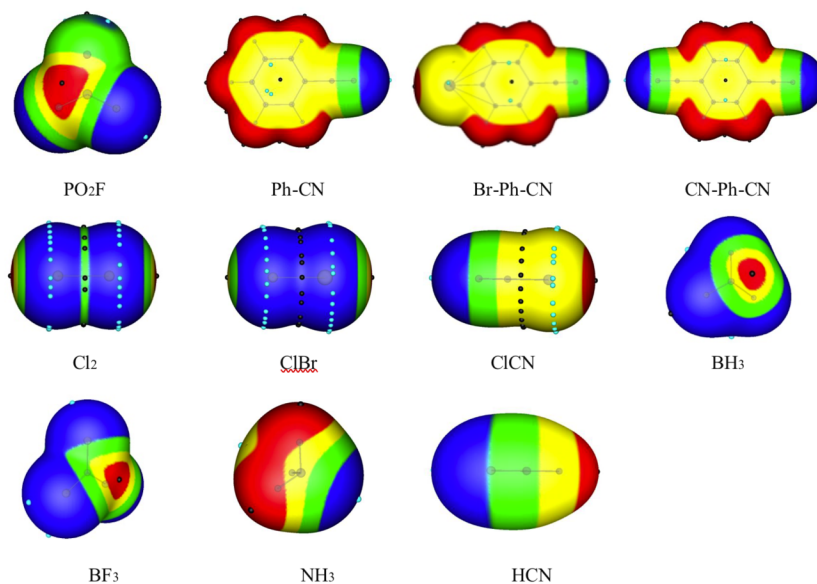


**Figure 1.** Molecular electrostatic potential maps at the 0.001 electron/ $\text{Bohr}^3$  isodensity surface of some representative isolated molecules in this study. The electrostatic potential varies from negative (blue) to neutral (green) and further to positive (red). The black and blue dots are surface maxima and minima, respectively.

**Table 1.** Molecular electrostatic potentials extrema (in kcal mol<sup>-1</sup>) on the 0.001 a.u. contour of the electron density ( $V_{s,max}$  and  $V_{s,min}$ ) of the isolated monomers.

Monomer <sup>a</sup>	$V_{s, min}$	Monomer <sup>a</sup>	$V_{s,max}$
Ph-CN*	-38.78	P*O <sub>2</sub> F	61.59
F-Ph-CN*	-37.05	Br*-Ph-CN	20.48
Cl-Ph-CN*	-36.63		
Br-Ph-CN*	-36.54		
CN-Ph-CN*	-32.23		
CH <sub>3</sub> -Ph-CN*	-40.25		
NH <sub>2</sub> -Ph-CN*	-43.49		
HCN*	-32.44		

<sup>a</sup> The atoms marked with asterisks are the reactive atoms with the extrema given in the table.

### 3.1.2 Geometries and Interactions

The schematic diagram for structure of the binary complex with pnictogen bonding is displayed in Figure 2, and the optimized geometries of these R-Ph-CN...PO<sub>2</sub>F complexes are shown in Figure S2, in which PO<sub>2</sub>F is approximately perpendicular to the R-Ph-CN molecular frame, and R denotes one of the several substituents chosen in this study. Since our interest is the study of the *para*-substitution effect and cooperativity effect on the pnictogen bonding, some other structures which may exist for R-Ph-CN...PO<sub>2</sub>F complex are not considered here anymore. The structures can be understood with the following MEP analysis of the molecules.

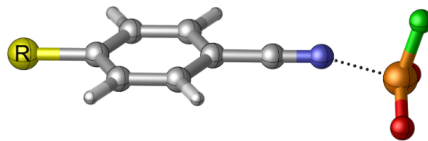


**Figure 2 .** Structure of the pnictogen bonding binary complex (R-Ph-CN...PO<sub>2</sub>F).

The geometry and the complexation energy of the considered binary systems are given in Table 2. The nonlinear C-N...P structure is due to the fact that the most positive MEP of the  $\pi$  hole of PO<sub>2</sub>F locates at the P-F bond closing to the P atom. Furthermore, upon formation of the  $\pi$ -hole pnictogen bond, the PO<sub>2</sub>F molecule deviates from the original planar structures, which is described by the following deformation energy. The pnictogen bond distance  $r(N...P)$  (the distance between N and P atoms) of Ph-CN...PO<sub>2</sub>F complex is 1.924 Å, much smaller than the sum of van der Waals (vdW) radii of N and P atoms (3.35 Å)<sup>[50]</sup>, indicating the existence of intermolecular interactions in the studied systems. When the *para*-H atom in Ph-CN is replaced by different substituents, it is found that the distance between N and P decreases for the -CH<sub>3</sub> and -NH<sub>2</sub> complexes, while the distance becomes larger for the halogen atom and CN group. As seen in Table

2, the pnicoen-bond length  $r(\text{N}\dots\text{P})$  decrease following the order of  $\text{CN} > \text{Br}[\text{?}]\text{Cl} > \text{F} > \text{H} > \text{CH}_3 > \text{NH}_2$ , which is consistent with the order of the  $V_{s, \text{min}}$  on the N atom of isolated substituted R-Ph-CN observed in the MEP analysis.

**Table 2.** The geometric and energetic aspects of the binary complexes (energy unit: kcal/mol).

Complex	$r(\text{N}\dots\text{P}) / \text{\AA}$	[?]P-O-O-F / degree	[?]F-P-O-O / degree	$\Delta E_{\text{bin}}^a / \text{kcal}\cdot\text{mol}^{-1}$	$\Delta E_{\text{int}}^a / \text{kcal}\cdot\text{mol}^{-1}$	$E_{\text{def}}^a / \text{kcal}\cdot\text{mol}^{-1}$
Ph-CN...PO <sub>2</sub> F	1.924	154.71	147.40	-19.25	-26.85	7.60
F-Ph-CN...PO <sub>2</sub> F	1.928	154.98	147.75	-18.84	-26.27	7.43
Cl-Ph-CN...PO <sub>2</sub> F	1.930	155.04	147.82	-18.52	-25.88	7.36
Br-Ph-CN...PO <sub>2</sub> F	1.930	155.04	147.82	-18.47	-25.82	7.35
CN-Ph-CN...PO <sub>2</sub> F	1.954	156.30	149.37	-16.57	-23.20	6.63
CH <sub>3</sub> -Ph-CN...PO <sub>2</sub> F	1.914	154.14	146.70	-20.09	-28.07	7.98
NH <sub>2</sub> -Ph-CN...PO <sub>2</sub> F	1.889	152.65	144.89	-22.22	-31.65	9.43
HCN...PO <sub>2</sub> F	2.097	—	155.77	-12.69	-16.74	4.05

<sup>a</sup>  $\Delta E_{\text{bin}}$ ,  $\Delta E_{\text{int}}$ , and  $E_{\text{def}}$  refers to the total binding energy, interaction energy, and the deformation energy of the binary complex obtained at the B2PLYP-D3/jun-cc-pVTZ level of theory. Energies are given with the BSSE correction.

The interaction energy ( $\Delta E_{\text{int}}$ ) and the binding energy ( $\Delta E_{\text{bin}}$ ) of Ph-CN...PO<sub>2</sub>F amount to -26.85 and -19.25 kcal/mol, respectively, which is stronger than those of HCN...PO<sub>2</sub>F complex (-16.74 and -12.69 kcal/mol) obtained at the same level (B2PLYP-D3/jun-cc-pVTZ). This is also consistent with the negative MEPs on the N end of HCN (-32.44 kcal/mol) and that of Ph-CN (-38.98 kcal/mol) calculated at B3LYP-D3/6-311+G(d,p) level, which may be attributed to the conjugative effect of the phenyl ring in Ph-CN. Although the actual values of  $\Delta E_{\text{int}}$  and  $\Delta E_{\text{bin}}$  are different for the studied complexes, the order of the relative energy for the complexes is same, with the stability of the binary complexes increases in the order of  $\text{CN} < \text{Br}[\text{?}]\text{Cl} < \text{F} < \text{H} < \text{CH}_3 < \text{NH}_2$ . This could possibly be explained by the fact that the nature of the substituent attached to the ring influence the electron density on the ring, thus affecting the binding energies of the complexes. The NH<sub>2</sub> group is a strong electron-donating substituent through positive resonance effect, and has a larger enhancing effect than the weak electron-donating CH<sub>3</sub> group which has both positive induction effect and hyperconjugation effect. The halogen substituents (F, Cl, Br), however, exert a negative induction effect and positive resonance effect to the R-Ph-CN molecule, and the calculated N...P distance and interaction energies indicate that the former is dominated for all the halogen substituents. All the halogen atoms are shown as electron-withdrawing substituents and weaken the pnicoen bond in comparison with Ph-CN...PO<sub>2</sub>F complexes. It is noted that the order of Lewis basicity of R-Ph-CN ( $\text{Br} < \text{Cl} < \text{F}$ ) does not agree with the electronegativity increase trend for halogen substituents. For example, for the Cl-Ph-CN...PO<sub>2</sub>F and F-Ph-CN...PO<sub>2</sub>F complexes, the stronger bonding occurs for the later species. This may be arising from the larger conjugative effect through the lone pair of the Cl atom with the  $\pi$  electron of the aromatic ring, which results in the greater  $V_{s, \text{min}}$  on the N atom of F-Ph-CN and larger interaction in the F-Ph-CN...PO<sub>2</sub>F complexes.

By examining the interaction energies  $\Delta E_{\text{int}}$  and the  $V_{\text{min}}$  on the N atom of the substituted R-Ph-CN derivatives, it can be seen that the strength of the interaction of the binary complexes increases as the

absolute value of  $V_{\min, N}$  become larger. In fact, as shown in Figure 3, an acceptable linear correlation is found between the  $\Delta E_{\text{int}}$  with  $V_{\min, N}$  values with a coefficient of determination  $R^2=0.961$ , which suggests the electrostatically driven nature of the pnictogen bonding interaction in stabilizing these complexes. Besides, according to the geometrical analysis, a good linear relationship exists between the binding energies  $\Delta E_{\text{int}}$  and the N...P intermolecular distance  $r(\text{N}\dots\text{P})$  with  $R^2=0.996$ , as can be seen in Figure 4(a).

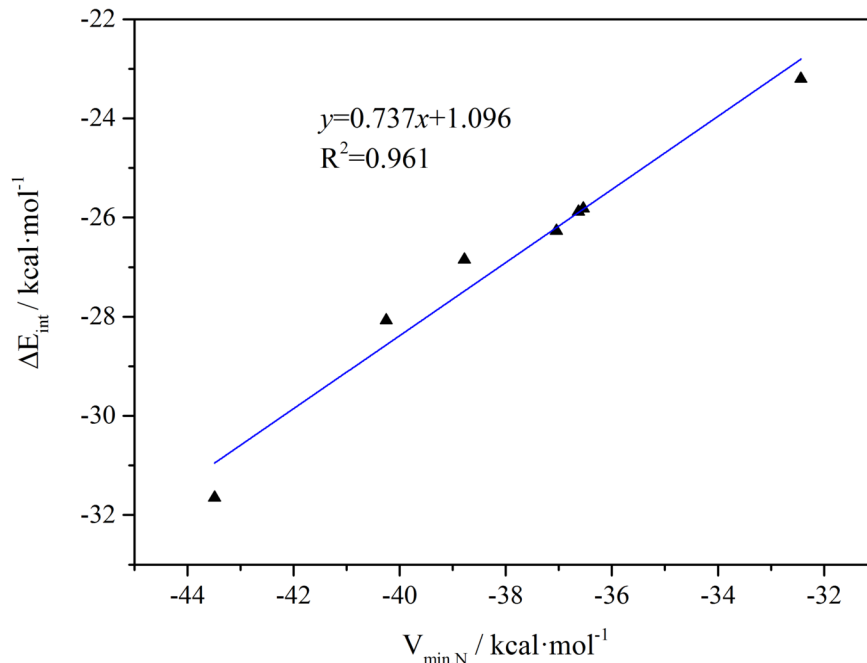
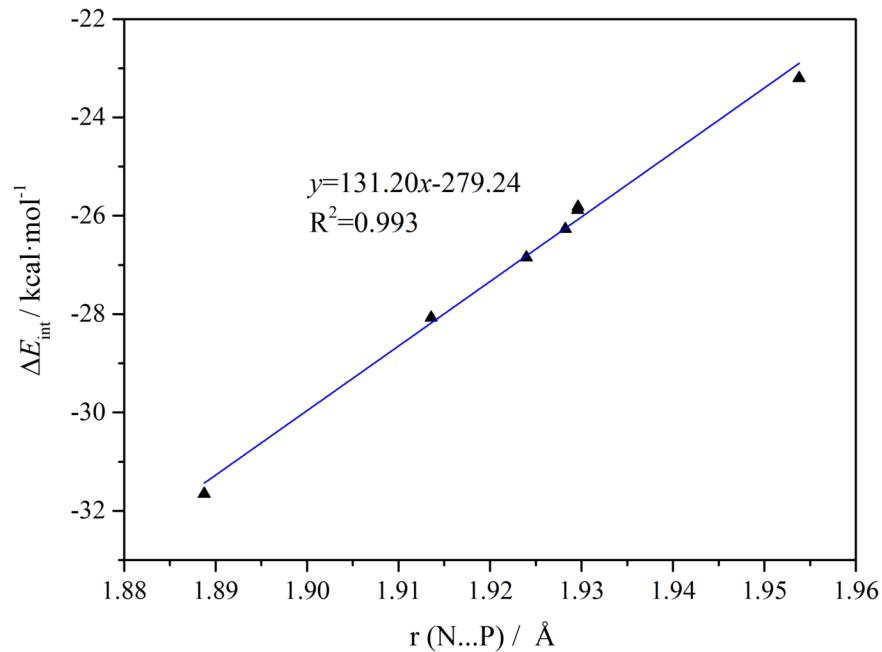
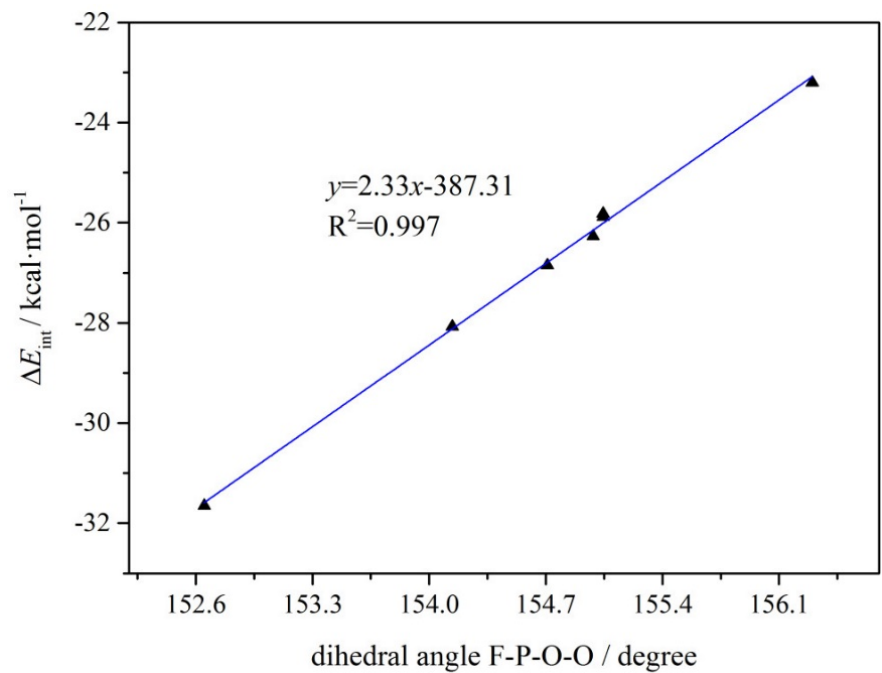


**Figure 3** . Linear relationship between the interaction energy  $\Delta E_{\text{int}}$  and  $V_{\min}$  values on the N atom of R-Ph-CN derivatives.

As for the deformation energy  $E_{\text{def}}$ , which is defined as the energy required to distort each monomer from its optimized structure to that within the complex, its contribution is prominent in the studied pnictogen-bonded complexes, being about 28-30% of the interaction energy. According to the optimized geometries of the complexes, the relative magnitude for the structural deformation upon complexation can be estimated by the variation of the dihedral angle F-P-O-O of the  $\text{PO}_2\text{F}$  molecule, which is  $180^\circ$  and  $147.4^\circ$  in the isolated monomer and Ph-CN... $\text{PO}_2\text{F}$  complex, respectively. The angle becomes smaller when the *para*-H atom in Ph-CN is replaced by the  $\text{CH}_3$  or  $\text{NH}_2$  group, while the changes are the contrary when the substituent is F, Cl, Br, or CN group. As displayed in Figure 4(b), a good linear relationship is observed between the interaction energy of the complex and the dihedral angle of F-P-O-O with  $R^2=0.997$ . It should be mentioned that in the earlier study of  $\text{XO}_2\text{F}\dots\text{NCH}$  and  $\text{XO}_2\text{F}\dots\text{CNH}$  ( $\text{X}=\text{P}, \text{As}$ ) by Zhuo *et al.*<sup>[51]</sup>, the deformation of the complexes is estimated by the changes of F-X...N/C angle. However, in our study, the linear correlation between the changes of P-O...N angle and the interaction energy of the complexes is not so good as that of the dihedral angle F-P-O-O of the  $\text{PO}_2\text{F}$  molecule. This indicates that the well-chosen geometrical parameters of the complexes can be used to nicely reflect and describe the strength of the intermolecular interaction.



(a)



(b)

**Figure 4.** Relationship between interaction energy and the geometrical parameters in R-Ph-CN...PO<sub>2</sub>F complexes, including (a) the N...P intermolecular distance  $r(\text{N}\dots\text{P})$ , and (b) the dihedral angle F-P-O-O.

### 3.1.3 AIM and NBO analyses

The quantum theory of AIM<sup>[52]</sup> is useful to analyze various intermolecular interactions. The N...P pnictogen bond is characterized by the existence of an intermolecular BCP between N atom of R-Ph-CN and the P atom of PO<sub>2</sub>F. Values of the corresponding topological parameters are gathered in Table 3. The Laplacian  $[\rho]^{(2)}$  of the BCPs are all positive, and this indicates a depletion of the electron density, which is common in closed-shell kind of interactions in the complexes<sup>[53]</sup>. It is known that the signs of  $[\rho]^{(2)}$  and  $H_{BCP}$  can be used to characterize the strength of intermolecular interaction and describe the covalent properties of a bond<sup>[54]</sup>. In the complexes studied herein, the positive  $[\rho]^{(2)}$  and negative  $H_{BCP}$  at the P...N BCP in all cases indicate that the P...N pnictogen bonding can be classified as medium strength interaction with partially covalent characteristics<sup>[55]</sup>. It is observed from Table 3 that the value of  $H_{BCP}$  become more negative, as the interaction energy of R-Ph-CN...PO<sub>2</sub>F increases, indicating the more covalent character in the P...N interactions. As seen in Figure 5, there is a good linear relationship between binding distance  $r(N...P)$  and bond critical point electron density ( $\rho_{N...P}$ ). Therefore, it is accepted that the electron density at the BCPs is a good measurement to estimate the strength of the pnictogen bond of the complexes we studied. Similar results have been observed in some H-bonded complexes, but it is the logarithm of the electron density that participated in the linear relationship<sup>[56]</sup>.

**Table 3.** The AIM topological parameters at the N...P BCPs and the natural bond orbital analysis of the R-Ph-CN...PO<sub>2</sub>F binary complexes.

Complex	$\rho_b$	$[\rho]^{(2)}$	$G_b$	$V_b$	$H_b$	$-G_b/V_b$	$E^{(2)}(1)^a$	$E^{(2)}(2)^a$	$q(PO_2F)^b$
Ph-CN...PO <sub>2</sub> F	0.0959	0.0358	0.0744	-0.1397	-0.0654	0.5321	114.15	5.09	-0.193
F-Ph-CN...PO <sub>2</sub> F	0.0951	0.0323	0.0725	-0.1370	-0.0645	0.5295	111.28	5.04	-0.190
Cl-Ph-CN...PO <sub>2</sub> F	0.0949	0.0316	0.0720	-0.1362	-0.0641	0.5290	110.80	5.04	-0.189
Br-Ph-CN...PO <sub>2</sub> F	0.0949	0.0316	0.0720	-0.1362	-0.0641	0.5290	110.84	5.04	-0.189
CN-Ph-CN...PO <sub>2</sub> F	0.0905	0.0204	0.0635	-0.1219	-0.0584	0.5210	100.73	4.90	-0.176
CH <sub>3</sub> -Ph-CN...PO <sub>2</sub> F	0.0978	0.0432	0.0786	-0.1464	-0.0678	0.5369	118.91	5.14	-0.200
NH <sub>2</sub> -Ph-CN...PO <sub>2</sub> F	0.1029	0.0638	0.0896	-0.1632	-0.0736	0.5489	142.10	3.54	-0.216

<sup>a</sup>  $E^{(2)}(1)$  and  $E^{(2)}(2)$  represent the second-order perturbation energy due to the  $Lp(N) \rightarrow p^*(P)$  and  $Lp(N) \rightarrow \sigma^*(P-O)$  interaction, respectively.  $E^{(2)}$  is in kcal[?] $mol^{-1}$ , and all other values are in a.u.

<sup>b</sup>  $q(PO_2F)$  refers to the net natural population analysis (NPA) charge on the PO<sub>2</sub>F moiety, in unit of e.

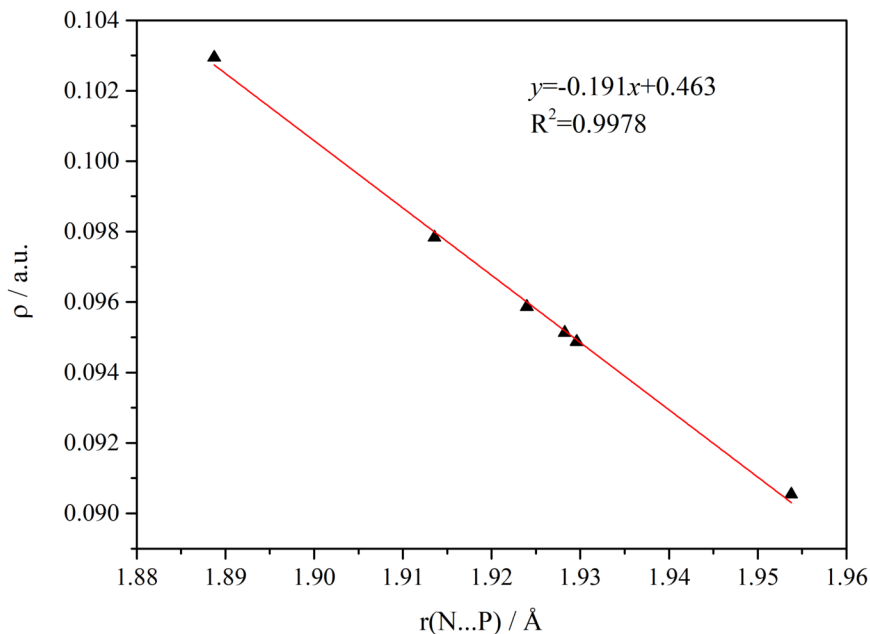
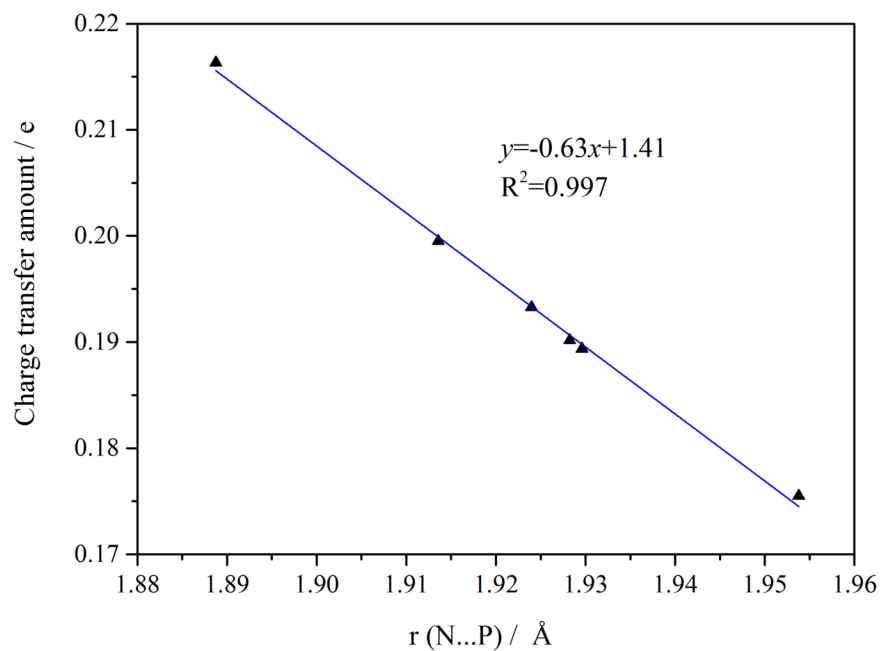
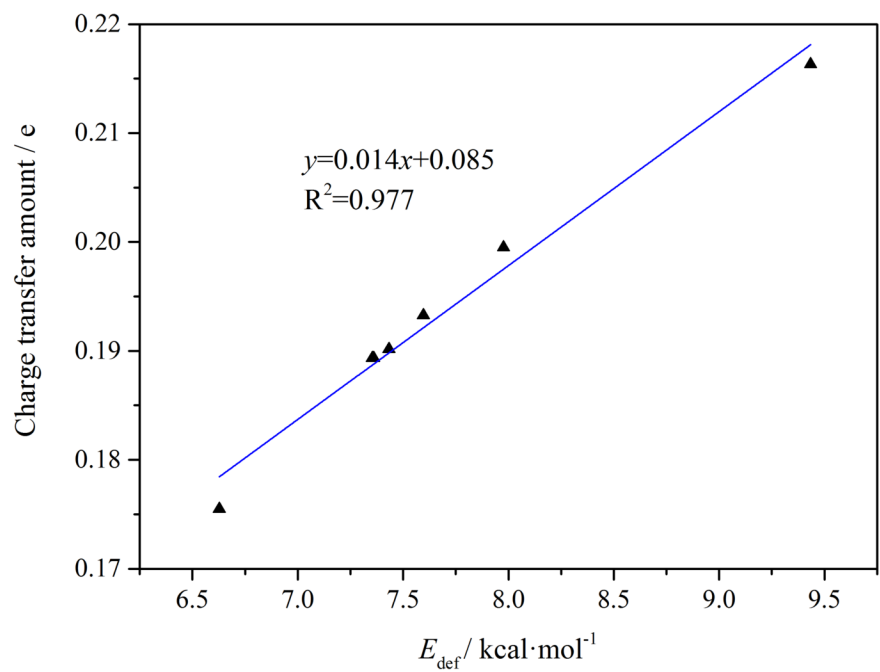


**Figure 5.** The linear correlation between intermolecular distance  $r(\text{N}\dots\text{P})$  and the electron density ( $\rho_b$ ) at  $\text{N}\dots\text{P}$  bond critical point in  $\text{R-Ph-CN}\dots\text{PO}_2\text{F}$  complexes.

The NBO analysis has been conducted to characterize the orbital-orbital interaction  $E^{(2)}$  and the charge transfer in the complexes studied herein, and the results are summarized in Table 3. As expected, there is an electron charge transfer shift from the Lewis base unit  $\text{R-Ph-CN}$  to the Lewis acid unit  $\text{PO}_2\text{F}$ . As a result,  $\text{PO}_2\text{F}$  gains electron density and becomes negatively charged, while  $\text{R-Ph-CN}$  base loses electron density and becomes positively charged. The charge transfer (CT) is expressed as the net natural population analysis (NPA) charge on all the atom of the electron donor molecule ( $\text{R-Ph-CN}$ ). As displayed in Figure 6(a), there is a good linear relationship between the total charge transfer amount and the binding distance  $r(\text{N}\dots\text{P})$  with  $R^2=0.997$ . The amount of charge transfer is 0.193 e for the  $\text{Ph-CN}\dots\text{PO}_2\text{F}$  complex, which is larger than the 0.125 e charge transfer computed for the  $\text{HCN}\dots\text{PO}_2\text{F}$  complex obtained at the same B3LYP-D3/6-311+G\*\* level. As pointed by Grabowski<sup>[38]</sup>, the deformation energy is strongly related to the electron charge transfer, which is often ignored in investigating the intermolecular interactions. Here, for the dimers we studied, an excellent linear relationship is found between the deformation energy and the charge transfer CT with  $R^2=0.977$ , as seen in Figure 6(b). For each complex, there are two dominant orbital interactions of  $\text{Lp}(\text{N})-\text{p}^*(\text{P})$  and  $\text{Lp}(\text{N})-\sigma^*(\text{P-O})$  in these pnictogen-bonded complexes, where  $\text{Lp}(\text{N})$  denotes the lone pair orbital on N atom, and  $\text{p}^*(\text{P})$  represents the empty  $\text{p}(\pi)$  orbital on P atom, and  $\sigma^*(\text{P-O})$  denotes the P-O antibonding orbital. The schematic diagrams of the orbital interactions in  $\text{Ph-CN}\dots\text{PO}_2\text{F}$  complex are displayed in Figure 7. As indicated from the second-order perturbation energies in the last three columns of Table 3, the contributions of the  $\text{Lp}(\text{N})-\text{p}^*(\text{P})$  orbital interaction ranges from 100.7 to 142.1 kcal/mol, which is far greater than that of  $\text{Lp}(\text{N})-\sigma^*(\text{P-O})$ . Similar to the case of tetrel bond<sup>[49]</sup>, this is a feature of strong pnictogen-bond. It is evident from Table 3 that the  $E^{(2)}$  energy of  $\text{R-Ph-CN}\dots\text{PO}_2\text{F}$  complexes follows the same order of the strength of the interactions.

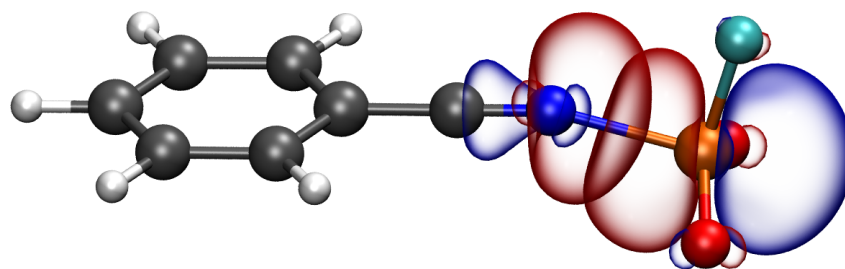


(a)

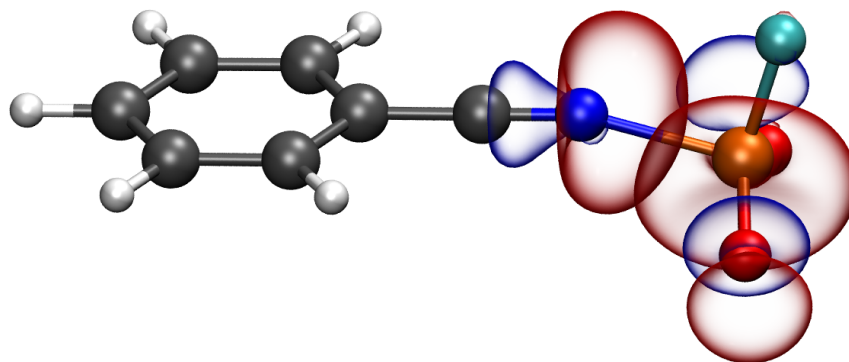


(b)

**Figure 6.** The linear relationship of the total charge transfer amount versus (a) the intermolecular distance  $r(\text{N}\dots\text{P})$  and (b) the deformation energy  $E_{\text{def}}$  (in kcal/mol) in R-Ph-CN...PO<sub>2</sub>F complexes.



(a)  $Lp(N) p^*(P)$



( $\beta$ )  $\Lambda\pi(N) \sigma^*(\Pi-O)$

**Figure 7 .** Schematic diagrams of the orbital interactions in Ph-CN...PO<sub>2</sub>F complex at the at the B3LYP-D3/6-311+G\*\* level.

## 3.2 Cooperative Effect Between pnictogen bond and halogen/triell bond

### 3.2.1 MEPs analysis

The MEP maps of the selected monomers in forming the ternary complexes X...CN-Ph-CN...PO<sub>2</sub>F and Y...Br-Ph-CN...PO<sub>2</sub>F for X=F<sub>2</sub>, Cl<sub>2</sub>, Br<sub>2</sub>, FCl, FBr, BrCl, FCN, ClCN, BrCN, BH<sub>3</sub>, BF<sub>3</sub>, and Y=NH<sub>3</sub>, NH<sub>2</sub>CH<sub>3</sub>, NHCH<sub>2</sub>, HCN are depicted in Figure 1 and Figure S1.

**Table 4.** The results of electrostatic potential analysis of the monomers and corresponding binary complexes (unit: kcal·mol<sup>-1</sup>)<sup>a</sup>

Monomer	$V_{\max}$ or $V_{\min}$	Complex	$V_{\min}$	$\Delta V_{\min}^b$
X...CN-Ph-CN	X...CN-Ph-CN	X...CN-Ph-CN	X...CN-Ph-CN	X...CN-Ph-CN
		CN-Ph-CN*	-32.23	0.00
F-F*	12.99	F <sub>2</sub> ...CN-Ph-CN*	-31.65	0.58
Cl-Cl*	25.59	Cl <sub>2</sub> ...CN-Ph-CN*	-30.69	1.54
Br-Br*	30.76	Br <sub>2</sub> ...CN-Ph-CN*	-30.15	2.09
F-Cl*	44.53	FCl...CN-Ph-CN*	-28.98	3.26
F-Br*	54.37	FBr...CN-Ph-CN*	-27.84	4.39

Monomer	$V_{\max}$ or $V_{\min}$	Complex	$V_{\min}$	$\Delta V_{\min}^b$
Br-Cl*	19.47	BrCl...CN-Ph-CN*	-31.26	0.97
Cl-Br*	36.94	ClBr...CN-Ph-CN*	-29.51	2.72
F*-CN	13.19	FCN...CN-Ph-CN*	-30.99	1.25
Cl*-CN	37.99	ClCN...CN-Ph-CN*	-29.81	2.42
Br*-CN	45.07	BrCN...CN-Ph-CN*	-29.14	3.10
B*H <sub>3</sub>	41.78	BH <sub>3</sub> ...CN-Ph-CN*	-28.53	3.71
B*F <sub>3</sub>	53.35	BF <sub>3</sub> ...CN-Ph-CN*	-26.02	6.22
<b>Z...Br-Ph-CN</b>	<b>Z...Br-Ph-CN</b>	<b>Z...Br-Ph-CN</b>	<b>Z...Br-Ph-CN</b>	<b>Z...Br-Ph-CN</b>
		Br-Ph-CN*	-36.54	0.00
N*H <sub>3</sub>	-40.44	NH <sub>3</sub> ...Br-Ph-CN*	-39.63	-3.09
N*H <sub>2</sub> CH <sub>3</sub>	-38.52	NH <sub>2</sub> CH <sub>3</sub> ...Br-Ph-CN*	-39.68	-3.14
N*H=CH <sub>2</sub>	-38.72	N*H=CH <sub>2</sub> ...Br-Ph-CN*	-39.54	-3.00
HCN	-32.44	HCN...Br-Ph-CN*	-39.40	-2.85

<sup>a</sup> For each molecule, the calculated  $V_{\max}$  or  $V_{\min}$  value refers to the atom marked with asterisk in the table.

<sup>b</sup>  $\Delta V_{\min}$  refers to the changes of the most negative MEP ( $V_{\min}$ ) on the free N atom in the binary complex relative to that of the corresponding monomer (CN-Ph-CN\* or Br-Ph-CN\*).

As shown in Figure 1, the two CN substituents in CN-Ph-CN make it to be a typical Lewis base due to its withdrawing nature. When R is substituted by Br atom, the MEPs maps of Br-Ph-CN possess a  $\sigma$ -hole on the extensions of the C-Br bond, which indicates that Br-Ph-CN can act as both Lewis acid and Lewis base. The  $V_{\max}$  and  $V_{\min}$  in these isolated monomers are gathered in Table 4. For the halogen-containing compounds, there are small positive electrostatic potential caps ( $\sigma$ -holes) on the outermost portion along the molecular axis, and these  $\sigma$ -holes represent the potential interaction sites with the Lewis base CN-Ph-CN. The calculated  $V_{\max}$  values for the halogen compounds ranges from 12.99 to 54.37 kcal/mol. For dihalogen compounds, the  $\sigma$ -hole values become more positive in the order  $F_2 < BrCl^* < Cl_2 < Br_2 < ClBr^* < FCl^* < FBr^*$ , and the atom which interact with CN-Ph-CN is denoted by an asterisk. As for BH<sub>3</sub> and BF<sub>3</sub>, two positive electrostatic potential regions exist along the vertical direction of the molecular plane ( $\pi$ -hole), corresponding to the location of the empty p orbital of the B atom, and thus a favorable triel bond with a Lewis base is expected for BH<sub>3</sub> and BF<sub>3</sub>. The value of  $V_{\max}$  is larger in BF<sub>3</sub> than that in BH<sub>3</sub>, which is in agreement with the earlier studies [44]. For the four nitrogen bases, blue regions with negative MEPs are found on the surface of the N atom, and the values of  $V_{\min,N}$  increase in the order  $HCN(sp) < NH_2CH_3(sp^3) < ([?])NHCH_2(sp^2) < NH_3(sp^3)$ , which is in accordance with the result obtained by Li *et al.* [57]

### 3.2.2 Geometries and Interactions of the Ternary complexes

Here, we will discuss the issue that when introducing the halogen or triel bond into the original binary complex, how the pnictogen bond will be affected by the interplay of these interactions. The optimized structures of some representative ternary complexes are plotted in Figure 8. The geometrical parameters and the interaction energies of the ternary and binary complexes are summarized in Table 5 and Table S1, respectively. For the trimolecular complexes X...CN-Ph-CN...PO<sub>2</sub>F, when X is the halides compounds (F<sub>2</sub>, Cl<sub>2</sub>, Br<sub>2</sub>, FCl, FBr, BrCl, ClBr, FCN, ClCN, BrCN), the free N atom in CN-Ph-CN interacts with the halides along the extension of C-N bond, forming halogen bonds, and when X is the boron-containing compound (BH<sub>3</sub>, BF<sub>3</sub>), the B...N(C) triel bonds will be formed. As for the ternary complexes of Y...Br-Ph-CN...PO<sub>2</sub>F, the Br atom interacts with the N-bases denoted by Y, including NH<sub>3</sub>, NH<sub>2</sub>CH<sub>3</sub>, NHCH<sub>2</sub>,

and HCN, with the formation of the N...Br halogen bond. The geometry of the P...N pnictogen bond is similar to that in the binary complexes, and the only difference is the P...N binding distance and the F-P-O-O dihedral angle, which indicate the strength of the pnictogen bond and the geometrical deformation upon formation of the ternary complexes, respectively.

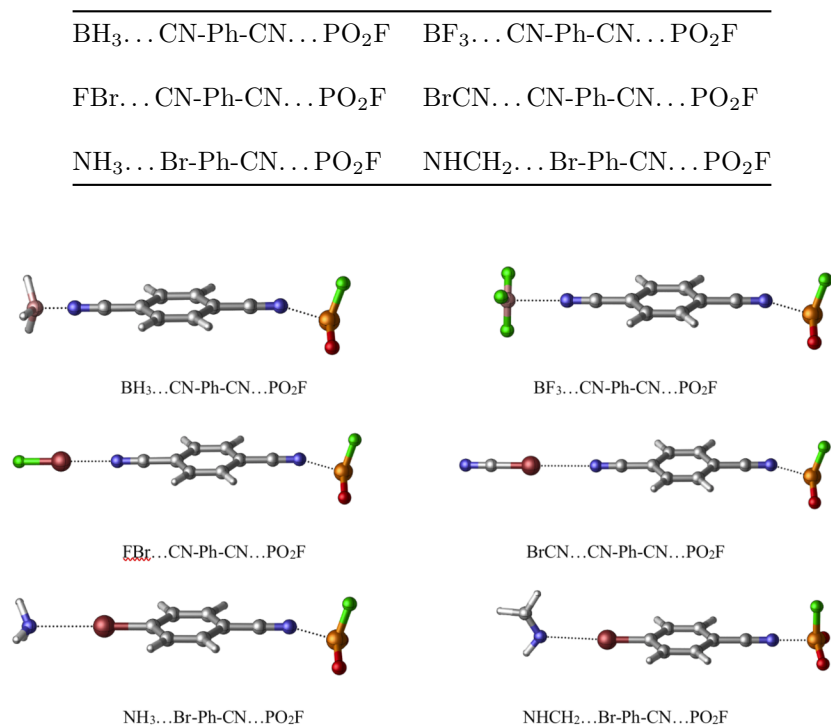


**Figure 8.** Optimized geometries of some representative ternary complexes obtained at the B3LYP-D3/6-311+G\*\* level of theory.

**Table 5.** The molecular geometric parameters and the energy information of the ternary complexes.

Complex	$r(X \dots N)^a$ / Å	$\Delta r(X \dots N)^b$ / Å	$r(N \dots P)$ / Å	$\Delta r(N \dots P)$ $b$ / Å	$\frac{\Delta r(X \dots N)}{\Delta r(N \dots P)}$ $c$	$\Delta E_{\text{bin}}^c$ / kcal·mol <sup>-1</sup>	$\Delta E_{\text{int}}^c$ / kcal·mol <sup>-1</sup>	$E_{\text{def}}^c$ / kcal·mol <sup>-1</sup>
F <sub>2</sub> ...CN- Ph- CN...PO <sub>2</sub> F	2.637	0.047	1.956	0.002	19.996	-17.60	-24.24	6.64
Cl <sub>2</sub> ...CN- Ph- CN...PO <sub>2</sub> F	2.791	0.049	1.960	0.006	7.690	-19.20	-25.84	6.64
Br <sub>2</sub> ...CN- Ph- CN...PO <sub>2</sub> F	2.838	0.056	1.963	0.009	6.232	-20.07	-26.62	6.55
FCl...CN- Ph- CN...PO <sub>2</sub> F	2.522	0.046	1.968	0.015	3.109	-21.60	-28.49	6.89
FBr...CN- Ph- CN...PO <sub>2</sub> F	2.475	0.037	1.974	0.020	1.874	-24.14	-31.11	6.97

Complex	$r(X \dots N)^a$ / Å	$\Delta r(X \dots N)^b$ / Å	$r(N \dots P)$ / Å	$\Delta r(N \dots P)$ <sup>b</sup> / Å	$\frac{\Delta r(X \dots N)}{\Delta r(N \dots P)}$ <sup>c</sup>	$\Delta E_{\text{bin}}^c$ / kcal·mol <sup>-1</sup>	$\Delta E_{\text{int}}^c$ / kcal·mol <sup>-1</sup>	$E_{\text{def}}^c$ / kcal·mol <sup>-1</sup>
BrCl... CN- Ph-	2.897	0.051	1.958	0.004	12.543	-18.64	-25.28	6.64
CN... PO <sub>2</sub> F								
ClBr... CN- Ph-	2.743	0.052	1.966	0.012	4.382	-20.86	-27.48	6.62
CN... PO <sub>2</sub> F								
FCN... CN- Ph-	3.071	0.028	1.958	0.005	6.239	-17.49	-23.98	6.49
CN... PO <sub>2</sub> F								
ClCN... CN- Ph-	3.005	0.034	1.964	0.010	3.405	-19.47	-25.83	6.36
CN... PO <sub>2</sub> F								
BrCN... CN- Ph-	2.973	0.039	1.967	0.013	2.984	-20.48	-26.79	6.31
CN... PO <sub>2</sub> F								
BH <sub>3</sub> ... CN- Ph-	1.537	-0.006	1.969	0.015	-0.414	-36.19	-57.00	20.81
CN... PO <sub>2</sub> F								
BF <sub>3</sub> ... CN- Ph-	2.405	0.581	1.967	0.013	45.637	-21.44	-29.14	7.70
CN... PO <sub>2</sub> F								
NH <sub>3</sub> ... Br- Ph-	2.965	-0.063	1.915	-0.014	4.451	-22.10	-30.01	7.91
CN... PO <sub>2</sub> F								
NH <sub>2</sub> CH <sub>3</sub> ... Br-	2.897	-0.065	1.915	-0.015	4.372	-22.87	-30.86	7.99
Ph-								
CN... PO <sub>2</sub> F								
HNCH <sub>2</sub> ... Br-	2.956	-0.068	1.914	-0.015	4.434	-22.08	-30.12	8.04
Ph-								
CN... PO <sub>2</sub> F								
HCN... Br- Ph-	3.129	-0.074	1.918	-0.012	6.314	-21.28	-29.09	7.81
CN... PO <sub>2</sub> F								

<sup>a</sup>  $r(X \dots N)$  represents the intermolecular distance between the boron / halogen atom and the nitrogen atom in the triel / halogen bonds of the ternary complexes, and X refers to the boron or halogen atom.

<sup>b</sup>  $\Delta r(X \dots N)$  and  $\Delta r(N \dots P)$  refers to the changes of the distance of  $r(X \dots N)$  and  $r(N \dots P)$  in ternary complexes relative to the binary complexes, respectively.

<sup>c</sup>  $\Delta r(X \dots N) / \Delta r(N \dots P)$  refers to the ratio between  $\Delta r(X \dots N)$  and  $\Delta r(N \dots P)$ .

<sup>d</sup>  $\Delta E_{\text{bin}}$ ,  $\Delta E_{\text{int}}$ , and  $E_{\text{def}}$  refers to the total binding energy, interaction energy, and the deformation energy of the ternary complex. Energies are given with the BSSE correction.

When forming trimolecular complexes of X...CN-Ph-CN...PO<sub>2</sub>F, all hal...N (hal=F, Cl, Br) and N...P distances in the trimers are larger than those in the dimers, which suggests that both halogen bond and pnictogen bond becomes weaker relative to the isolated bimolecular complexes. For example, the N...P distance in CN-Ph-CN...PO<sub>2</sub>F is 1.954 Å, and the Br...N distance in FBr...CN-Ph-CN is 2.438 Å. With

the formation of FBr...CN-Ph-CN...PO<sub>2</sub>F complex, the two distances are both elongated to 1.974 and 2.475 Å, respectively. In such type of ternary complexes, the elongation of the halogen bonding length is more prominent than the pnictogen bonding distance.

When the additional interaction is triel bond, the N...P distances X...CN-Ph-CN...PO<sub>2</sub>F increase to 1.969 and 1.967 Å for X=BH<sub>3</sub> and BF<sub>3</sub>, respectively. It can be seen that there is a clear change in the geometry for the B-containing molecule, which deviates from the planar trigonal structure in the isolated monomer to tetrahedral geometry in the complexes. This is also observed in several triel-bonded complexes<sup>[44, 49]</sup>, indicating strong  $\pi$ -hole triel bonding interaction. To confirm the reliability of the computational methods, we have also calculated the structures of BF<sub>3</sub>...HCN, and the results indicate that the B...N distance is predicted to be 2.408 Å at the B2PLYP-D3/6-311+G\*\*, which compares favorably with the data obtained from the microwave spectra experiment (2.473±0.029 Å)<sup>[58]</sup>. Here, for our selected system, the B...N distance is calculated to be 1.543 and 1.824 Å in BH<sub>3</sub>...CN-Ph-CN, and BF<sub>3</sub>...CN-Ph-CN complexes, respectively. The differences of the geometries between BH<sub>3</sub> and BF<sub>3</sub> systems here compare well with those of other nitrile...BH<sub>3</sub> complexes and their BF<sub>3</sub> counterparts<sup>[59]</sup>, which indicate that BF<sub>3</sub> complexes are weaker with longer B...N distance and smaller N...B-X angles. This is consistent with the earlier findings that BH<sub>3</sub> is a stronger Lewis acid than BF<sub>3</sub>, which is partly due to the backbonding effect<sup>[60]</sup>. When these two dimers form the trimers complexes with PO<sub>2</sub>F, one could expect that the B...N distance will become larger, as the CN-Ph-CN acts as Lewis acids in both triel bond and pnictogen bond in the complexes. But surprisingly, the observed changes are different from the expected behaviors. That is, the B...N distance is contracted to be 1.537 Å for the former and elongated to be 2.405 Å for the latter, although the N...P distances become larger in both complexes in comparison with the CN-Ph-CN...PO<sub>2</sub>F dimer. To ensure the validity of the calculated unusual variation of the B...N distance, we have reoptimized the structure of the complexes at the wB97XD/6-311+G\*\* level, and the same trend is observed. That is, the value of B...N distance decreases from 1.559 Å in dimer to 1.552 Å in trimer for the BH<sub>3</sub>-involving complexes, while it increases from 1.814 Å in dimer to 2.422 Å in trimer for the BF<sub>3</sub>-involving complexes. Besides, it is worth mentioning that for the halogen bonded binary complexes in the research systems, as shown in Table S1, the proportion of the deformation energy  $E_{\text{def}}$  is smaller than 15% of the binding energy, while for the triel bonded binary complex,  $E_{\text{def}}$  is similar to or even much greater than the binding energy, and for BF<sub>3</sub>...CN-Ph-CN complex,  $E_{\text{def}}$  is approximately three times greater than the binding energy. However, upon formation of the ternary complexes, the deformation for the BF<sub>3</sub>-involving trimolecular complexes become smaller than those of BH<sub>3</sub> complexes, with the angle of F-B...N changing from 101.10° in dimer to 93.53° in trimer. The deformation is large if the angle has a larger derivation with 90°. These changes may be arising from the influence of the pnictogen bond in the ternary complex.

When the additional N...Br halogen bond is formed by introducing the nitrogen bases into the Br-Ph-CN...PO<sub>2</sub>F complexes, the binding distance of N...Br and N...P are both shortened in comparison with those in binary complex, which indicates that both halogen bond and pnictogen bond are reinforced from binary to ternary complexes. As seen from both the binding energy and interaction energy, the strength of the halogen bonding between the N-bases and Br-Ph-CN increase in the sequence HCN<NH<sub>3</sub><NHCH<sub>2</sub><NH<sub>2</sub>CH<sub>3</sub>, which is inconsistent with the values of  $V_{\text{min,N}}$  from the ESP analysis.

### 3.2.3 Cooperative Energy

The total interaction energy ( $\Delta E$  (ABC) or  $\Delta E_{\text{total}}$ ) and the cooperative energy  $E_{\text{coop}}$ , as well as the two-body terms are all summarized in Table 6, which are obtained at B2PLYP/jun-cc-pVTZ level for all studied systems. The values of  $E_{\text{coop}}$  are positive for X...CN-Ph-CN...PO<sub>2</sub>F trimers, and this means that the strength of both halogen (or triel) bonding and pnictogen bonding interaction decrease upon the formation of the ternary complexes, which is also termed as the negative synergistic effect or diminutive effect<sup>[60]</sup>. When the halogen bond is introduced into CN-Ph-CN...PO<sub>2</sub>F complexes, the  $E_{\text{coop}}$  ranges from 0.23 to 2.01 kcal/mol for the systems we studied. As for the Y...Br-Ph-CN...PO<sub>2</sub>F, the negative  $E_{\text{coop}}$  values reveal that the interactions are strengthened in trimer in comparison with the sum of the halogen bonding and the pnictogen bonding interactions in dimers, and this can be called positive synergistic effect. The  $E$

$E_{\text{coop}}$  corresponds to -1.32 to -1.65 kcal/mol. These findings related to the cooperative effect are consistent with the variations of the intermolecular distance as discussed above. As displayed in Figure 9, it is interesting to find that the ratio of the changes of the halogen bonding distance to the changes of the pnictogen bonding distance, i.e.  $\Delta r(\text{hal}\dots\text{N})/\Delta r(\text{N}\dots\text{P})$ , show exponential correlation with the cooperative energy  $E_{\text{coop}}$ , and the correlation coefficient  $R^2$  is 0.927. This indicates that, for two given type of the interactions, the greater the cooperative effect, the smaller for the difference between the variations of the two interaction distances.

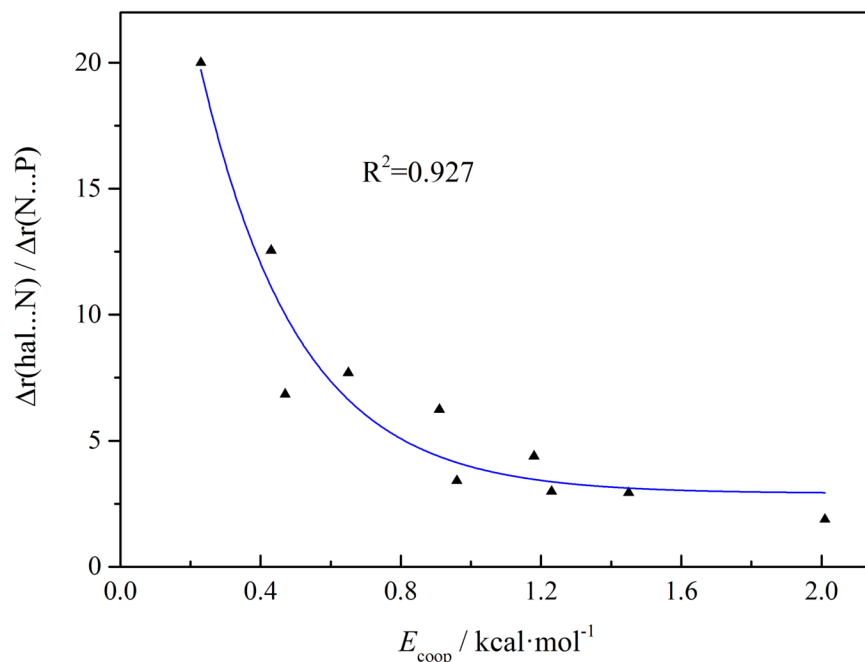


**Figure 9** . Exponential correlations between the cooperative energy  $E_{\text{coop}}$  and the ratio of changes of the halogen bonding distance to the changes of the pnictogen bonding distance  $\Delta r(\text{hal}\dots\text{N})/\Delta r(\text{N}\dots\text{P})$ .

Since the pnictogen bonding is the same in the trimer, the cooperative energy varies depending on the strength in  $\text{X}\dots\text{CN-Ph-CN}$  or  $\text{Y}\dots\text{Br-Ph-CN}$ . In most cases, the cooperative effect becomes more prominent when the additional interaction in  $\text{X}\dots\text{CN-Ph-CN}$  or  $\text{Y}\dots\text{Br-Ph-CN}$  is larger. As can be seen in Figure 10, a good linear relationship is found between the halogen bonding interaction in  $\text{X}\dots\text{CN-Ph-CN}$  ( $\text{X}=\text{dihalogen compounds, including } \text{F}_2, \text{Cl}_2, \text{Br}_2, \text{FCl, FBr, BrCl, ClBr}$ ) and the percentage of  $E_{\text{coop}}$  to the total interaction energy  $\Delta E_{\text{total}}$ . The  $E_{\text{coop}}$  decrease in the order of  $\text{F}_2 < \text{BrCl}^* < \text{Cl}_2 < \text{Br}_2 < \text{ClBr}^* < \text{FCl}^* < \text{FBr}^*$ , which is in good agreement with the order of  $V_{\text{max}}$  values of the  $\sigma$ -hole on the halogen atoms as discussed above. Combined with the studies of Zhang *et al.*<sup>[44]</sup>, it is found that the cooperative energy and its percentage to  $\Delta E_{\text{total}}$  are both smaller when the benzenoid derivatives are served as the bridge molecule than the heterocyclic systems. This may be due to the fact that the mutual effect of the interaction is weakened through the aromaticity of phenyl ring, while the strength is still very strong through the bond of the heterocyclic ring. Therefore, the interplay between the two interaction is strongly influenced by bonding characteristic of the bridge molecule, in addition to the strength of both interactions.

**Table 6.** The total interaction in the ternary complex ( $[?]E(\text{ABC})$ ), the interaction energy of the halogen/triyl bond ( $[?]E(\text{AB})$ ) and pnictogen bond ( $[?]E(\text{BC})$ ), and cooperative energy ( $E_{\text{coop}}$ ) in the ternary complexes (Unit: Kcal/mol).

Complex	$[?]E(\text{AB})$	$[?]E(\text{BC})$	$[?]E(\text{ABC})$	$[?]E(\text{A-C})_{\text{far}}$	$[?][?]E(\text{AB})$	$[?][?]E(\text{BC})$	$E_{\text{coop}}$
$\text{F}_2 \dots \text{CN-Ph-CN} \dots \text{PO}_2\text{F}$	-1.27	-23.20	-24.24	0.00	0.16	0.24	0.23

Complex	[?]E(AB)	[?]E(BC)	[?]E(ABC)	[?]E(A-C) <sub>far</sub>	[?][?]E(AB)	[?][?]E(BC)	$E_{\text{coop}}$
Cl <sub>2</sub> ... CN-Ph-CN... PO <sub>2</sub> F	-3.30	-23.20	-25.84	0.01	0.48	0.67	0.65
Br <sub>2</sub> ... CN-Ph-CN... PO <sub>2</sub> F	-4.34	-23.20	-26.62	0.01	0.67	0.90	0.91
FCl... CN-Ph-CN... PO <sub>2</sub> F	-6.77	-23.20	-28.49	0.03	1.08	1.36	1.45
FBr... CN-Ph-CN... PO <sub>2</sub> F	-9.96	-23.20	-31.11	0.04	1.51	1.91	2.01
BrCl... CN-Ph-CN... PO <sub>2</sub> F	-2.51	-23.20	-25.28	0.00	0.32	0.44	0.43
ClBr... CN-Ph-CN... PO <sub>2</sub> F	-5.48	-23.20	-27.48	0.02	0.88	1.16	1.18
FCN... CN-Ph-CN... PO <sub>2</sub> F	-1.28	-23.20	-23.98	0.03	0.37	0.49	0.47
ClCN... CN-Ph-CN... PO <sub>2</sub> F	-3.63	-23.20	-25.83	0.04	0.73	1.00	0.96
BrCN... CN-Ph-CN... PO <sub>2</sub> F	-4.87	-23.20	-26.79	0.05	0.92	1.28	1.23
BH <sub>3</sub> ... CN-Ph-CN... PO <sub>2</sub> F	-35.85	-23.20	-57.00	0.03	1.64	1.86	2.02
BF <sub>3</sub> ... CN-Ph-CN... PO <sub>2</sub> F	-19.41	-23.20	-29.14	0.02	13.13	1.24	13.45
NH <sub>3</sub> ... Br-Ph-CN... PO <sub>2</sub> F	-2.57	-25.82	-30.01	-0.05	-1.18	-1.75	-1.57
NH <sub>2</sub> CH <sub>3</sub> ... Br-Ph-CN... PO <sub>2</sub> F	-3.34	-25.82	-30.86	-0.05	-1.24	-1.83	-1.65
HNCH <sub>2</sub> ... Br-Ph-CN... PO <sub>2</sub> F	-2.92	-25.82	-30.12	-0.06	-1.18	-1.54	-1.32
HCN... Br-Ph-CN... PO <sub>2</sub> F	-1.8	-25.82	-29.09	-0.06	-1.08	-1.49	-1.41

<sup>a</sup> [?]E (AB), [?]E (BC), and [?]E (ABC) are the interaction energies of A...B, B...C, A...B...C complexes, respectively. [?]E (A-C)<sub>far</sub> is the interaction energy between two unbonded molecules in the A...B...C ternary system. [?][?]E is the difference of [?]E in the ternary complex relative to the corresponding binary complex.

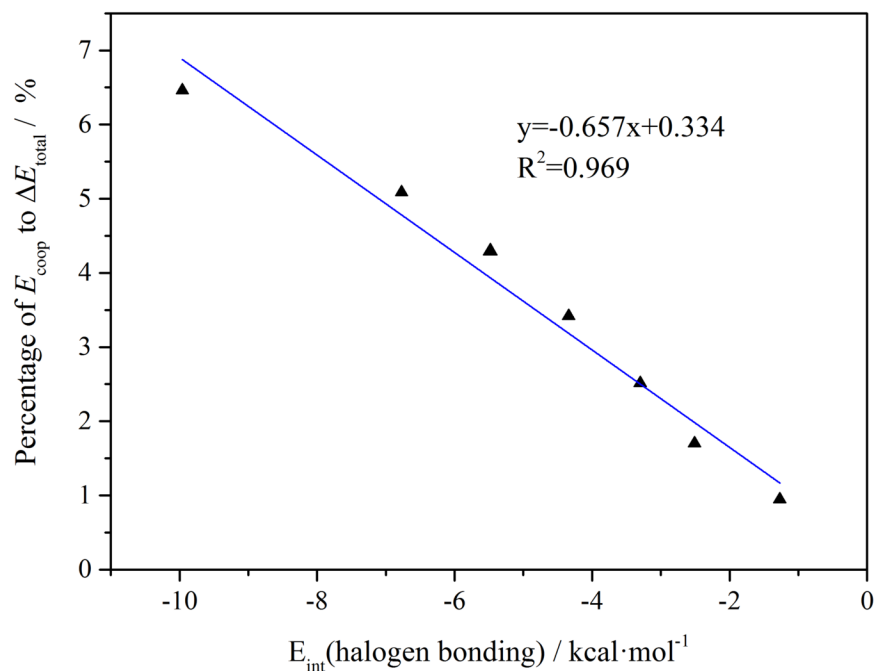


**Figure 10.** The linear relationship between the interaction energy of the halogen bonding in dimer and the percentage of  $E_{\text{coop}}$  to the total interaction of trimer.

When X is BH<sub>3</sub>, although the B...N distance shows a slight contraction upon the formation of trimer which is opposite to that expected, the interaction energy between BH<sub>3</sub> and CN-Ph-CN vary as expected, from -35.85 kcal/mol in the case of BH<sub>3</sub>...CN-Ph-CN dimer decreasing to -34.21 kcal/mol for BH<sub>3</sub>...CN-Ph-CN...PO<sub>2</sub>F

trimer. Similar inconsistent changes of structural parameter and the interaction energy have been obtained in earlier investigations of a series of  $\text{RCN}\dots\text{BH}_3$  complexes<sup>[59]</sup>. The calculated results *via* MP2/aug-cc-pVTZ indicated that the binding energies are 17.4 and 22.6 kcal/mol for  $\text{F}_3\text{CCN}\dots\text{BH}_3$  and  $\text{CH}_3\text{CN}\dots\text{BH}_3$ , while the corresponding B...N distance is 1.576 and 1.584 Å, respectively. It is counterintuitive that the electron-withdrawing substituent on the nitrile exhibits shorter distances. Herein, similar cases occur in the  $\text{BH}_3$  complexes. That is, the shorter B...N distances in the trimer compared to that in dimer is also contrary to the expectation, given CN-Ph-CN acts as both Lewis base in the two interactions in the complex. We attribute the observation to the inductive effect on the spacial extent of the *sp* lone pair of the N atom, *i.e.*, the negative synergistic effect of the pnictogen bond in CN-Ph-CN... $\text{PO}_2\text{F}$  results in the lone pair contracts, and the optimal overlap can only be achieved at even shorter B...N distances. When X is  $\text{BF}_3$ , however, the B...N distance varies in the expected manner, *i.e.*, uniformly increasing with the binding energies decreasing. The different behaviors shown by  $\text{BH}_3$  and  $\text{BF}_3$  upon formation of the trimers may be due to the greater  $\pi$  electron density on the  $\text{BF}_3$  moiety<sup>[59]</sup>, which interacts more strongly with the  $\pi$  electron density with CN-Ph-CN. The resulted different Pauli repulsion can be used to explain the different structural variations between the complexes of the  $\text{BH}_3$  and  $\text{BF}_3$ .

In order to deeply understand the interplay between the two interactions in the ternary complexes, the most negative MEP ( $V_{\min}$ ) on the free N atom in X...CN-Ph-CN and Y...Br-Ph-CN dimers, and the changes of  $V_{\min}$  ( $\Delta V_{\min}$ ) in comparison with that in CN-Ph-CN (-32.23 kcal/mol) and Br-Ph-CN (-36.54 kcal/mol) monomers are summarized in Table 4. The  $V_{\min}$  on the free N atom decreases in all the X...CN-Ph-CN dimers, and thus it forms a weaker pnictogen bond in the X...CN-Ph-CN... $\text{PO}_2\text{F}$  complexes. On the other hand, the increasing  $V_{\min}$  on the free N atom in the Y...Br-Ph-CN dimer enables Br-Ph-CN to be a stronger base in forming the ternary complexes. Furthermore, a good linear correlation between the  $\Delta V_{\min}$  and the cooperative energy  $E_{\text{coop}}$  has been found with  $R^2=0.991$ , as shown in Figure 11, except for the values of the  $\text{BF}_3\dots\text{CN-Ph-CN}$  dimer. This suggests that the electrostatic interaction is the main driving force in forming the complexes. As for  $\text{BF}_3\dots\text{Br-Ph-CN}\dots\text{PO}_2\text{F}$ , the cooperative energy amounts to be 13.45 kcal/mol, which is largest among the systems we studied. This may be caused by the abnormal great geometrical changes upon formation of the ternary complexes, which has been described above.

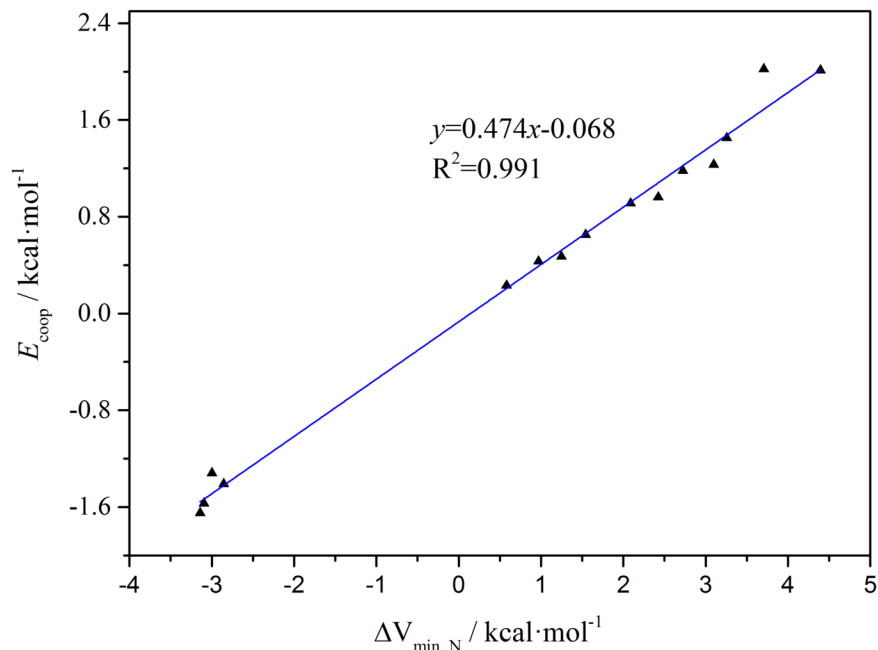


**Figure 11** . The linear relationship between the cooperative energy  $E_{\text{coop}}$  versus the changes of the

changes of  $V_{\min}$  ( $\Delta V_{\min}$ ) on the free N atom in X...CN-Ph-CN and Y...Br-Ph-CN dimers compared with the corresponding R-Ph-CN monomers.

### 3.2.4 AIM and NBO analyses

Table 7 presents the topological parameters in some representative dimers and trimers. The positive Laplacian  $[?]^2\rho_{\text{BCP}}$  and the negative  $H_{\text{BCP}}$  at the N...P and B...N BCPs indicate that both the pnictogen bonding and triel bonding belong to partially covalent interactions. The synergistic effect is also manifested in the changes of the electron density at the BCPs in the trimer in comparison with the dimers, since the  $\rho_{\text{BCP}}$  can be used to estimate the strength of the intermolecular interactions. The  $\rho_{\text{BCP}}$  at Hal...P (Hal=F, Cl, Br) and N...P BCPs decreases in X...CN-Ph-CN...PO<sub>2</sub>F complexes, while that at Br...N and N...P BCPs increases in the Y...Br-Ph-CN...PO<sub>2</sub>F complexes. These changes of  $\rho_{\text{BCP}}$  are consistent with the  $E_{\text{coop}}$  we obtained. Different variations occur for the BH<sub>3</sub>...CN-Ph-CN...PO<sub>2</sub>F and BF<sub>3</sub>...CN-Ph-CN...PO<sub>2</sub>F complexes. For the former, the  $\rho_{\text{BCP}}$  at B...N BCP increases from 0.0880 to 0.1186 a.u. in comparison with that in BH<sub>3</sub>...CN-Ph-CN dimer, while for the latter, it decreases from 0.0884 a.u. in dimer to 0.0216 a.u. in trimer. These B...N bonding changes are consistent with the variations of the B...N distance, which decreases from 1.543 to 1.537 Å for the former, and increase from 1.824 to 2.405 Å for the latter, respectively.

**Table 7.** The AIM topological analysis of some representative binary and ternary complexes (Unit: a.u.)

Complex	BCP	$\rho_b$	$[?]^2\rho_b$	$G_b$	$V_b$	$H_b$	$-G_b/V_b$
<b>CN-Ph-CN...PO<sub>2</sub>F</b>	N...P	0.0905	0.0204	0.0635	-0.1219	-0.0584	0.5210
BrCl...CN-Ph-CN	Cl...N	0.0147	0.0581	0.0122	-0.0098	0.0024	1.2403
BrCl...CN-Ph-CN...PO <sub>2</sub> F	N...P	0.0899	0.0188	0.0622	-0.1196	-0.0575	0.5196
	Cl...N	0.0131	0.0524	0.0109	-0.0086	0.0022	1.2584
ClBr...CN-Ph-CN	Br...N	0.0234	0.0826	0.0185	-0.0163	0.0022	1.1348
ClBr...CN-Ph-CN...PO <sub>2</sub> F	N...P	0.0886	0.0167	0.0597	-0.1153	-0.0556	0.5181
	Br...N	0.0208	0.0752	0.0165	-0.0142	0.0023	1.1602
BH <sub>3</sub> ...CN-Ph-CN	B...N	0.1172	0.6804	0.2330	-0.2959	-0.0629	0.7874
BH <sub>3</sub> ...CN-Ph-CN...PO <sub>2</sub> F	N...P	0.0880	0.0159	0.0587	-0.1135	-0.0548	0.5175
	B...N	0.1186	0.6988	0.2384	-0.3020	-0.0637	0.7892
BF <sub>3</sub> ...CN-Ph-CN	B...N	0.0708	0.0923	0.0673	-0.1115	-0.0442	0.6035
BF <sub>3</sub> ...CN-Ph-CN...PO <sub>2</sub> F	N...P	0.0884	0.0166	0.0595	-0.1149	-0.0554	0.5181
	B...N	0.0216	0.0643	0.0160	-0.0159	0.0001	1.0042
<b>Br-Ph-CN...PO<sub>2</sub>F</b>	N...P	0.0949	0.0316	0.0720	-0.1362	-0.0641	0.5290
NH <sub>3</sub> ...Br-Ph-CN	N...Br	0.0148	0.0450	0.0100	-0.0088	0.0012	1.1415
NH <sub>3</sub> ...Br-Ph-CN...PO <sub>2</sub> F	N...P	0.0975	0.0419	0.0778	-0.1452	-0.0674	0.5360
	N...Br	0.0167	0.0502	0.0113	-0.0100	0.0013	1.1269
HCN...Br-Ph-CN	N...Br	0.0084	0.0313	0.0063	-0.0048	0.0015	1.3060
HCN...Br-Ph-CN...PO <sub>2</sub> F	N...P	0.0970	0.0399	0.0768	-0.1435	-0.0668	0.5347
	N...Br	0.0098	0.0362	0.0074	-0.0057	0.0017	1.2878

The NBO analysis was performed to get an insight into the interplay between pnictogen bonding and other interactions. The results of the NBO analysis are summarized in Table S2. One can see that CT is much larger in the pnictogen bond than that in the halogen bond, while it is smaller in the pnictogen bond than that in the triel bond. It is generally accepted that the larger CT corresponds to a stronger interaction<sup>[49]</sup>, although for different types of interaction there is no good correlation between CT and binding energies. It is observed that the charge transfer is reduced for both the halogen bond and pnictogen bond in X...CN-Ph-CN...PO<sub>2</sub>F complexes, and a reverse result is found in Y...Br-Ph-CN...PO<sub>2</sub>F complexes. It should be mentioned that in the case of BH<sub>3</sub>...CN-Ph-CN and BH<sub>3</sub>...CN-Ph-CN...PO<sub>2</sub>F systems, the complexes are considered as one molecule in the NBO program, and thus the relevant charge transfer energies  $E^{(2)}$  were not

obtained. For  $\text{BF}_3 \dots \text{CN-Ph-CN}$  and  $\text{BF}_3 \dots \text{CN-Ph-CN} \dots \text{PO}_2\text{F}$  systems, N lone pair donation occurs from the Lewis base into the empty  $p(\pi)$  orbital of B. The  $E^{(2)}$  greatly decreases from 152.28 to 14.93 kcal/mol from dimer to the trimer, which is consistent with the increased B...N distance in the trimer in comparison with the dimer.

## 4 Conclusions

In this paper, theoretical calculations have been carried out for the binary and ternary complexes involving the substituted benzonitrile and  $\text{PO}_2\text{F}$  to study how the substituent and cooperative effect tune the  $\pi$ -hole pnictogen bonding interaction. In the binary complexes of  $\text{R-Ph-CN} \dots \text{PO}_2\text{F}$ , it is found that these pnictogen bonds can be classified as medium strength interaction, possessing partially covalent characteristics, and the stability of the complexes increases with respect to substituent R in the order of  $\text{CN} < \text{Br} < \text{Cl} < \text{F} < \text{H} < \text{CH}_3 < \text{NH}_2$ . The electron-donating ability of the substituent adjoined with the benzene ring give rise to an increase of the interaction energy of the complexes. All the halogen atoms behave as electron-withdrawing substituents and weaken the pnictogen bond compared with  $\text{Ph-CN} \dots \text{PO}_2\text{F}$  complexes. The geometrical analysis indicates that the dihedral angle F-P-O-O of the  $\text{PO}_2\text{F}$  molecule in the complexes can well describe the strength of the intermolecular interaction. The bonding nature of the intermolecular interactions has been further explored by means of AIM and NBO methods. As for the ternary complexes, the mutual interplay between pnictogen bond and halogen bond indicated that the negative/positive synergistic effect is consistent with the geometrical changes and cooperative energy upon formation of the trimer. The effect of a pnictogen bond on a halogen bond is more pronounced than that of a halogen bond on a pnictogen bond. The results indicated that the interplay between the two interaction is strongly influenced by bonding characteristic of the bridge molecule, in addition to the strength of both interactions. When the ternary complexes contain triel bond, however, notable differences are observed for  $\text{BH}_3$  and  $\text{BF}_3$ , including structural parameter and the interaction energy, which may be arising from the greater  $\pi$  electron density on the  $\text{BF}_3$  moiety. The MEP, AIM and NBO methodologies are used to analyze the nature of mutual interactions of the complexes. It is hoped that the results of our study are useful in a deep understanding of the nature of  $\pi$ -hole pnictogen bonding and how to tune it in more complex systems.

## Conflicts of interest

There are no conflicts to declare.

## Funding Information

This work was supported by the Natural Science Foundation of Shandong Province under Grant No. ZR2017MB023 and No. ZR2016BL09; and the Research Fund of Binzhou University under Grant No. BZXLYG1919.

## Supporting Information

Additional supporting information may be found online in the Supporting Information section at the end of the article.

## References

- [1] H.-J. Schneider, *Angew. Chem. Int. Edit.* , **2009** , *48* , 3924.
- [2] M. Giese, M. Albrecht, K. Rissanen, *Chem. Commun.* , **2016** , *52* , 1778.
- [3] K. T. Mahmudov, M. N. Kopylovich, M. da Silva, A. J. L. Pombeiro, *Coordin. Chem. Rev.* , **2017** , *345* , 54.
- [4] A. J. Neel, M. J. Hilton, M. S. Sigman, F. D. Toste, *Nature* , **2017** , *543* , 637.
- [5] A. C. Legon, *Phys. Chem. Chem. Phys.* , **2017** , *19* , 14884.
- [6] S. Scheiner, *Acc. Chem. Res.* , **2013** , *46* , 280.
- [7] J. Schmauck, M. Breugst, *Organic & Biomolecular Chemistry* , **2017** , *15* , 8037.
- [8] S. Zahn, R. Frank, E. Hey-Hawkins, B. Kirchner, *Chem. Eur. J.* , **2011** , *17* , 6034.
- [9] K. Eskandari, N. Mahmoodabadi, *J. Phys. Chem. A* , **2013** , *117* , 13018.
- [10] M. D. Esrafil, A. Sadr-Mousavi, *J. Mol. Graph. Model.* , **2017** , *75* , 165.
- [11] A. Mohajeri, K. Eskandari, S. A. Safae, *New J. Chem.* , **2017** , *41* , 10619.
- [12] M. D. Esrafil, P. Mousavian, *Mol. Phys.* , **2018** , *116* , 526.
- [13] Y. Li, Z. F. Xu, *J. Mol. Model.* , **2018** , *24* , 9.
- [14] W. Zierkiewicz, M. Michalczyk, S. Scheiner, *Phys. Chem. Chem. Phys.* , **2018** , *20* , 8832.
- [15] M. D. Esrafil, P. Mousavian, F. Mohammadian-Sabet, *Mol. Phys.* , **2019** , *117* , 58.
- [16] H. Lin, L. Meng, X. Li, Y. Zeng, X. Zhang, *New J. Chem.* , **2019** , *43* , 15596.
- [17] J. S. Murray, P. Lane, P. Politzer, *Int. J. Quantum. Chem.* , **2007** , *107* , 2286.
- [18] J. S. Murray, P. Lane, T. Clark, K. E. Riley, P. Politzer, *J. Mol. Model.* , **2012** , *18* , 541.
- [19] I. Alkorta, J. Elguero, J. E. Del Bene, *J. Phys. Chem. A* , **2013** , *117* , 10497.
- [20] A. Bauzá, R. Ramis, A. Frontera, *J. Phys. Chem. A* , **2014** , *118* , 2827.
- [21] A. Bauza, A. Frontera, *ChemPhysChem* , **2015** , *16* , 3108.
- [22] S. Scheiner, *Int. J. Quantum. Chem.* , **2013** , *113* , 1609.
- [23] U. Adhikari, S. Scheiner, *Chem. Phys. Lett.* , **2012** , *536* , 30.
- [24] I. Alkorta, F. Blanco, P. M. Deyà, J. Elguero, C. Estarellas, A. Frontera, D. Quiñonero, *Theor. Chem. Acc.* , **2010** , *126* , 1.
- [25] A. S. Mahadevi, G. N. Sastry, *Chem. Rev.* , **2016** , *116* , 2775.
- [26] H. Y. Zhuo, Q. Z. Li, W. Z. Li, J. B. Cheng, *New J. Chem.* , **2015** , *39* , 2067.
- [27] J. E. Del Bene, I. Alkorta, J. Elguero, G. Sanchez-Sanz, *J. Phys. Chem. A* , **2017** , *121* , 1362.
- [28] R. Wysokinski, W. Zierkiewicz, M. Michalczyk, S. Scheiner, *J. Phys. Chem. A* , **2020** , *124* , 2046.
- [29] A. Mukherjee, S. Tothadi, G. R. Desiraju, *Acc. Chem. Res.* , **2014** , *47* , 2514.
- [30] S. J. Grabowski, *ChemPhysChem* , **2015** , *16* , 1470.
- [31] M. J. Frisch, G. W. Trucks, H. B. Schlegel, G. E. Scuseria, M. A. Robb, J. R. Cheeseman, G. Scalmani, V. Barone, G. A. Petersson, H. Nakatsuji, X. Li, M. Caricato, A. V. Marenich, J. Bloino, B. G. Janesko, R.

- Gomperts, B. Mennucci, H. P. Hratchian, J. V. Ortiz, A. F. Izmaylov, J. L. Sonnenberg, Williams, F. Ding, F. Lipparini, F. Egidi, J. Goings, B. Peng, A. Petrone, T. Henderson, D. Ranasinghe, V. G. Zakrzewski, J. Gao, N. Rega, G. Zheng, W. Liang, M. Hada, M. Ehara, K. Toyota, R. Fukuda, J. Hasegawa, M. Ishida, T. Nakajima, Y. Honda, O. Kitao, H. Nakai, T. Vreven, K. Throssell, J. A. Montgomery Jr., J. E. Peralta, F. Ogliaro, M. J. Bearpark, J. J. Heyd, E. N. Brothers, K. N. Kudin, V. N. Staroverov, T. A. Keith, R. Kobayashi, J. Normand, K. Raghavachari, A. P. Rendell, J. C. Burant, S. S. Iyengar, J. Tomasi, M. Cossi, J. M. Millam, M. Klene, C. Adamo, R. Cammi, J. W. Ochterski, R. L. Martin, K. Morokuma, O. Farkas, J. B. Foresman, D. J. Fox, Gaussian 16 Revision. A.03, Gaussian Inc., Wallingford, CT, **2016** .
- [32] T. Schwabe, S. Grimme, *Phys. Chem. Chem. Phys.* , **2007** , *9* , 3397.
- [33] S. Grimme, S. Ehrlich, L. Goerigk, *J. Comput. Chem.* , **2011** , *32* , 1456.
- [34] P. D. Mezei, G. I. Csonka, A. Ruzsinszky, J. Sun, *J. Chem. Theory. Comput.* , **2015** , *11* , 360.
- [35] A. Forni, S. Pieraccini, D. Franchini, M. Sironi, *J. Phys. Chem. A* , **2016** , *120* , 9071.
- [36] L. Goerigk, A. Hansen, C. Bauer, S. Ehrlich, A. Najibi, S. Grimme, *Phys. Chem. Chem. Phys.* , **2017** , *19* , 32184.
- [37] E. Papajak, D. G. Truhlar, *J. Chem. Theory. Comput.* , **2011** , *7* , 10.
- [38] S. J. Grabowski, *Phys. Chem. Chem. Phys.* , **2017** , *19* , 29742.
- [39] S. J. Grabowski, *J. Comput. Chem.* , **2018** , *39* , 472.
- [40] S. F. Boys, F. Bernardi, *Mol. Phys.* , **1970** , *19* , 553.
- [41] J. C. White, E. R. Davidson, *J. Chem. Phys.* , **1990** , *93* , 8029.
- [42] Q. Li, Q. Lin, W. Li, J. Cheng, B. Gong, J. Sun, *ChemPhysChem* , **2008** , *9* , 2265.
- [43] M. Vatanparast, E. Parvini, A. Bahadori, *Mol. Phys.* , **2016** , *114* , 1478.
- [44] J. R. Zhang, W. Z. Li, J. B. Cheng, Z. B. Liu, Q. Z. Li, *Rsc Advances* , **2018** , *8* , 26580.
- [45] F. A. Bulat, A. Toro-Labbe, T. Brinck, J. S. Murray, P. Politzer, *J. Mol. Model.* , **2010** , *16* , 1679.
- [46] T. Lu, F. W. Chen, *J. Comput. Chem.* , **2012** , *33* , 580.
- [47] W. Humphrey, A. Dalke, K. Schulten, *J. Mol. Graph. Model.* , **1996** , *14* , 33.
- [48] E. D. Glendening, A. E. Reed, J. E. Carpenter, F. Weinhold, NBO Version 3.1.
- [49] H. Xu, J. Cheng, X. Yang, Z. Liu, X. Bo, Q. Li, *RSC Advances* , **2017** , *7* , 21713.
- [50] M. A. Dvorak, R. S. Ford, R. D. Suenram, F. J. Lovas, K. R. Leopold, *J. Am. Chem. Soc.* , **1992** , *114* , 108.
- [51] H. Y. Zhuo, Q. Z. Li, W. Z. Li, J. B. Cheng, *J. Chem. Phys.* , **2014** , *141* .
- [52] R. F. W. Bader, *Atoms in Molecules. A Quantum Theory.*, Clarendon Press, Oxford, U. K., **2000** .
- [53] R. F. W. Bader, *Chem. Rev.* , **1991** , *91* , 893.
- [54] W. D. Arnold, E. Oldfield, *J. Am. Chem. Soc.* , **2000** , *122* , 12835.
- [55] I. Alkorta, J. Elguero, S. J. Grabowski, *Phys. Chem. Chem. Phys.* , **2015** , *17* , 3261.
- [56] Y. X. Wei, J. B. Cheng, S. B. Yang, B. Xiao, Q. Z. Li, *Mol. Phys.* , **2018** , *116* , 1862.
- [57] M. X. Liu, Q. Z. Li, W. Z. Li, J. B. Cheng, *J. Mol. Graph. Model.* , **2016** , *65* , 35.
- [58] S. W. Reeve, W. A. Burns, F. J. Lovas, R. D. Suenram, K. R. Leopold, *J. Phys. Chem.* , **1993** , *97* , 10630.

- [59] E. L. Smith, D. Sadowsky, C. J. Cramer, J. A. Phillips, *J. Phys. Chem. A* , **2011** , *115* , 1955.
- [60] S. J. Grabowski, *ChemPhysChem* , **2014** , *15* , 2985.